Supplementary Materials

Supplementary Table S1.

Patient ID	Underlying disease	Type of LTx	Age, Sex	Rejection grade	Treatment	Complications	Time before retransplantation
126459	PAH	Heart-Lung	31, F	BOS III	Corticosteroids, Antibiotics	Aspergillus, Aureus	1 year
128308		Heart-Lung	F				6 years
128720	PAH, histiocytosis	SLTx	42, F			Edema, Staphylococcus, CMV infection	8 years
129053	PAH		41, F			Infection	2 years
129654	IPD	DLTx	33, M			Aspergillus, Fibrotic pneumopathy	7 years

Characteristics of the OB/BOS explanted lungs from the retransplanted patients used in this study.

List of supplementary figures.

Supplementary Figure S1. Single left lobe lung function after LTx.

Supplementary Figure S2. Pathological changes of the bronchial epithelium in the mismatched lung grafts.

Supplementary Figure S3. Expression and distribution of the HLA-A2 transgene in untouched and transplanted mouse lungs.

Supplementary Figure S4. Qualitative assessment of plasma autoantibodies following LTx.

Supplementary Figure S5. B cells infiltrating the allografts are of recipient origin.

Supplementary Figure S6. Percentages of T helper and B effector responses in MLN from lung transplanted mice.

Supplementary Figure S7. Intracellular IFNg and IL17A in MLNs of lung transplanted rejecting mice.

Supplementary Figure S8. The formation of GCs in MLN is dependent on the HLA mismatch and on EBI2.

Supplementary Figure S9. Ebi2 deficiency is associated with reduced B cell activation and follicle formation.

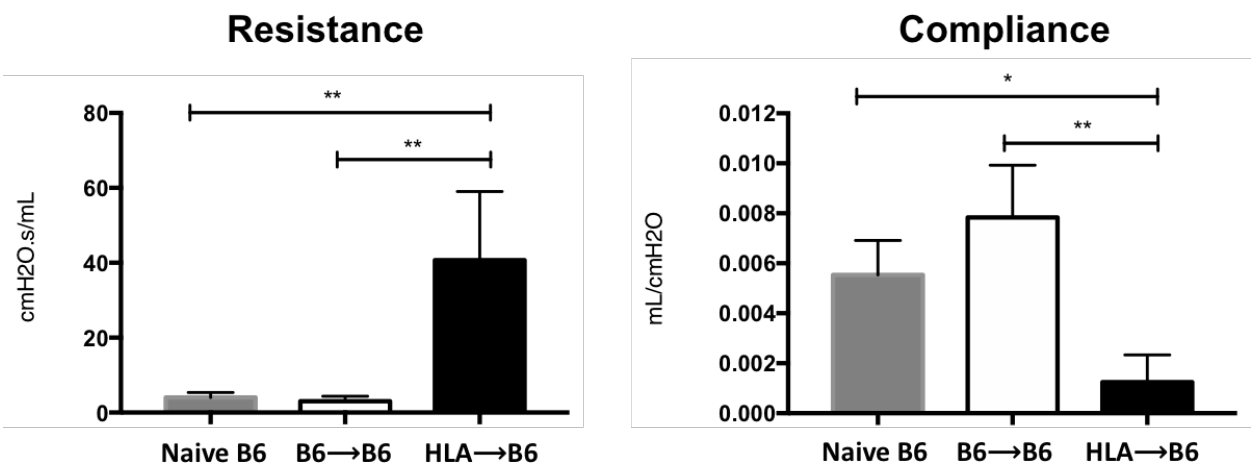

Fig S1. Single left lobe lung function after LTx. After clamping the right bronchus, lung function was measured in the left lobes from naïve B6 mice and the transplanted left lobes from B6→B6 and HLA→B6 mice 1 month after LTx. Left panel: left lobe resistance. Right panel: left lobe compliance. Data are expressed as mean+/-SEM and analyzed with a One-Way ANOVA, followed by a Tukey's post-test. **p*<0.05; **p*<0.01.

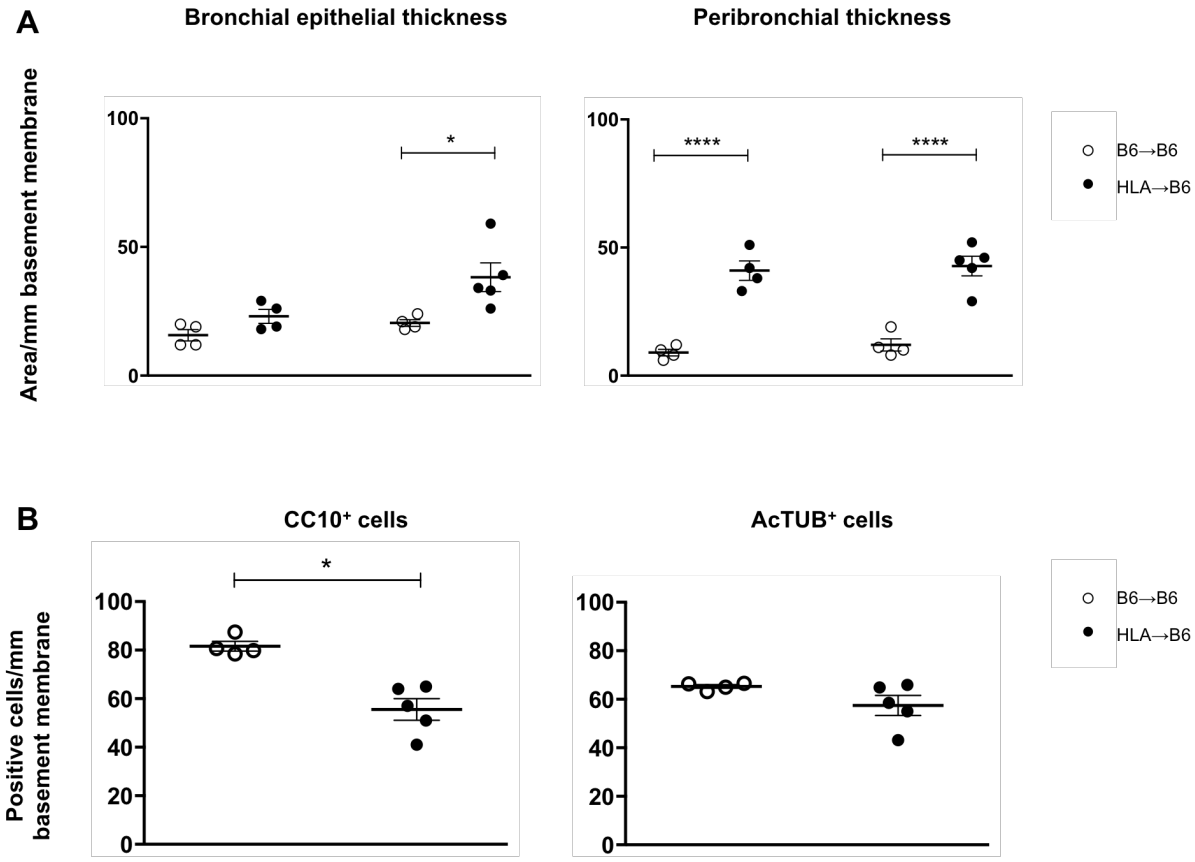

Fig S2. Pathological changes of the bronchial epithelium in the mismatched lung grafts. 2 months after lung transplantation, **(A)** the bronchial epithelial and peribronchial B6→B6 and HLA→B6, as well as (B) the CC10+ and AcTUB+ cell numbers were quantified. Data are expressed as mean+/-SEM and analyzed with a Two-Way ANOVA, followed by a Bonferroni post-test. *p<0.05; ****p<0.0001 (A), or with a Mann-Whitney test. *p<0.05 (B).

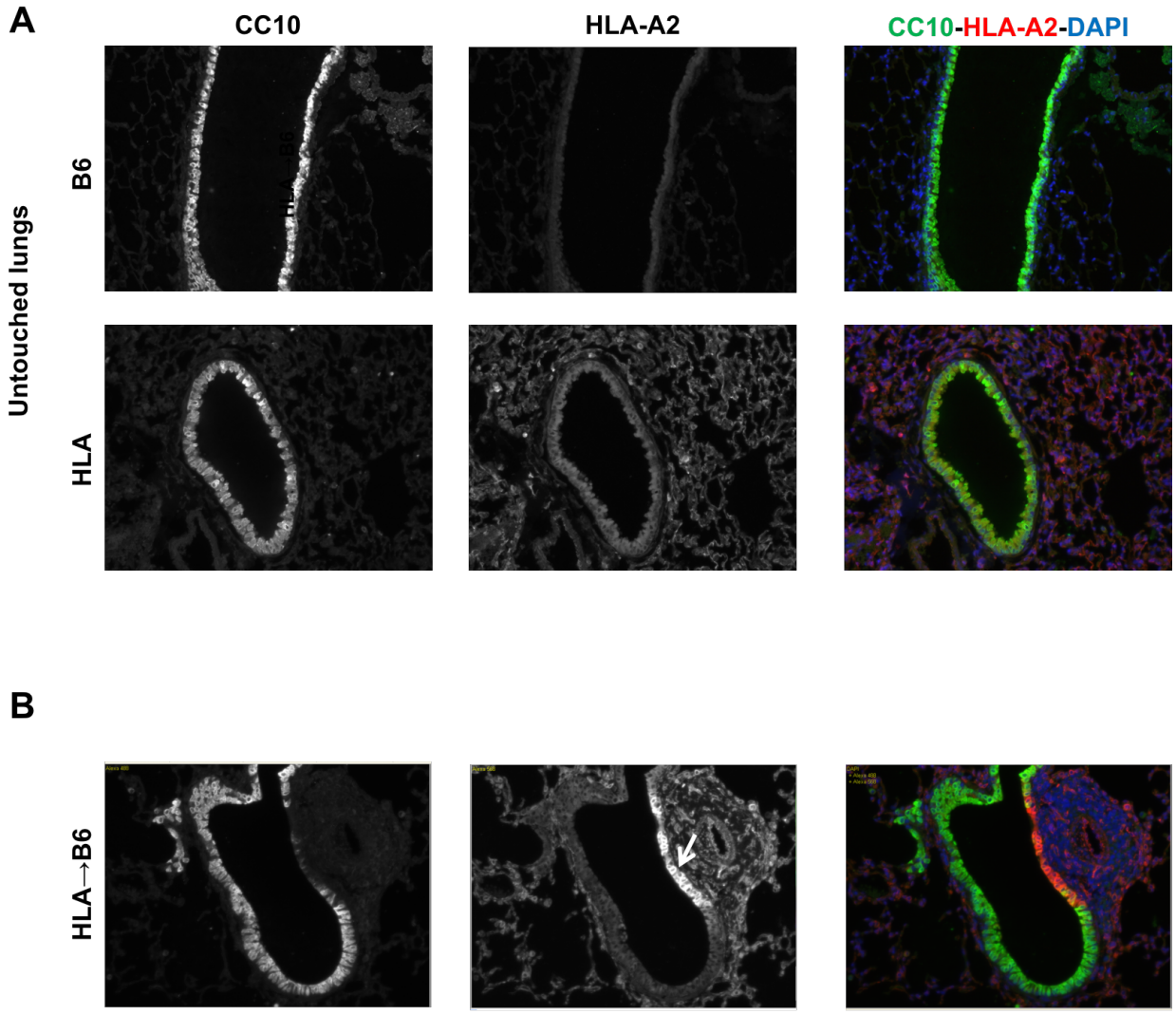

Fig S3. Expression and distribution of the HLA-A2 transgene in untouched and transplanted mouse lungs. Representative double immunofluorescence pictures of bronchi stained for CC10 (green) and HLA-A2 (red) from **(A)** untouched B6 and HLA mice, **(B)** HLAB6 mice 2 months after lung transplantation. Single channel and merged pictures. Magnification x20.

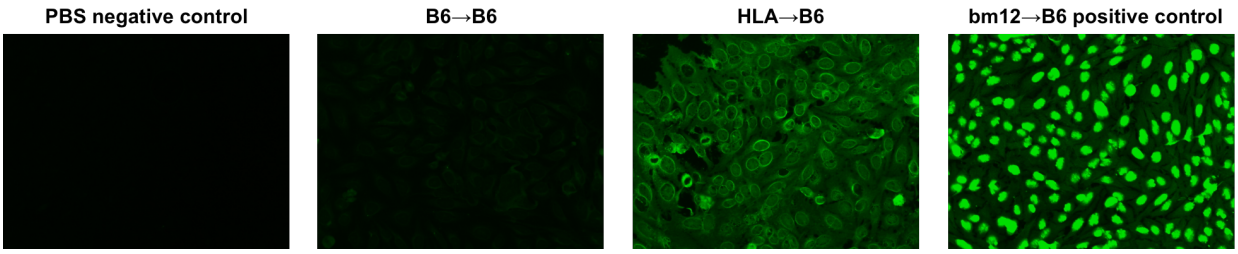

Fig S4. Qualitative assessment of plasma autoantibodies following LTx. Plasma collected from B6→B6, HLA→B6 and bm12→B6 (considered as a positive control) 2 months after lung transplantation was incubated on Hep-2 slides and autoantibodies were then detected with an anti-mouse FITC-conjugated antibody.

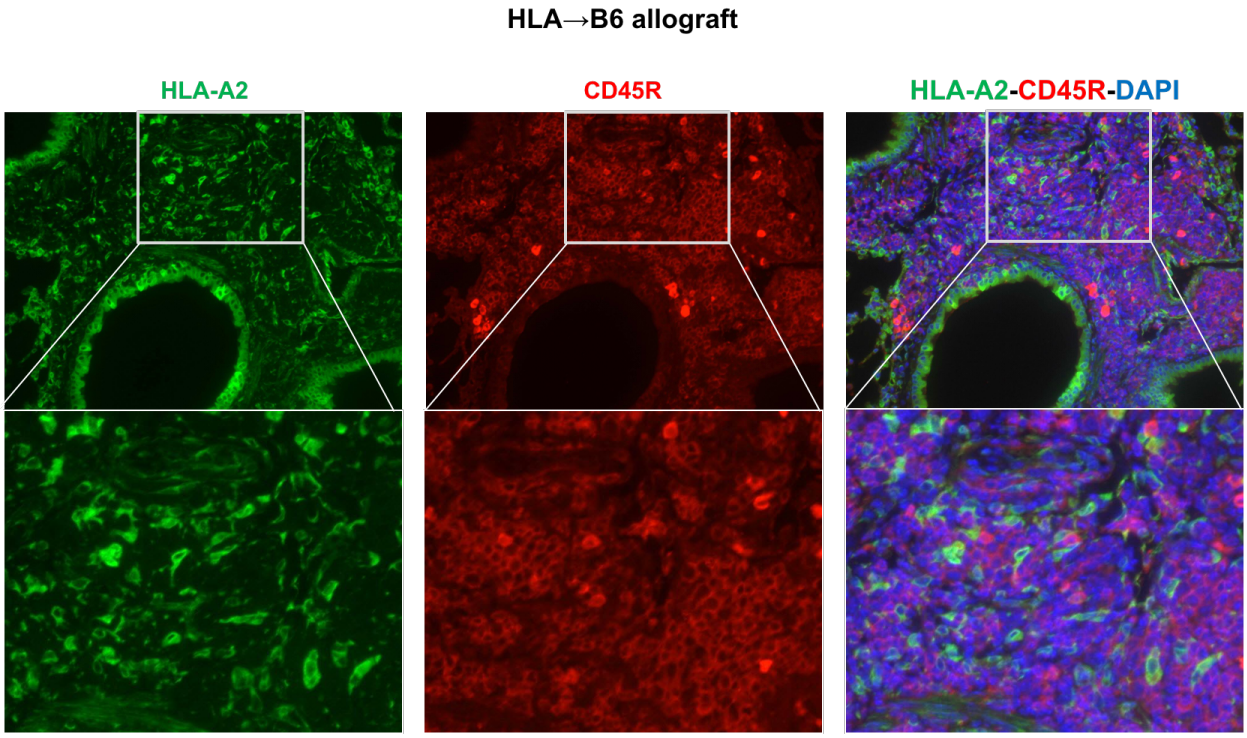

Fig S5. B cells infiltrating the allografts are of recipient origin. Representative double immunofluorescence pictures of bronchial areas from HLA→B6 mice 2 months after lung transplantation, stained for HLA-A2 (green) to identify donor-derived cells and for CD45R (red) to identify B cells.

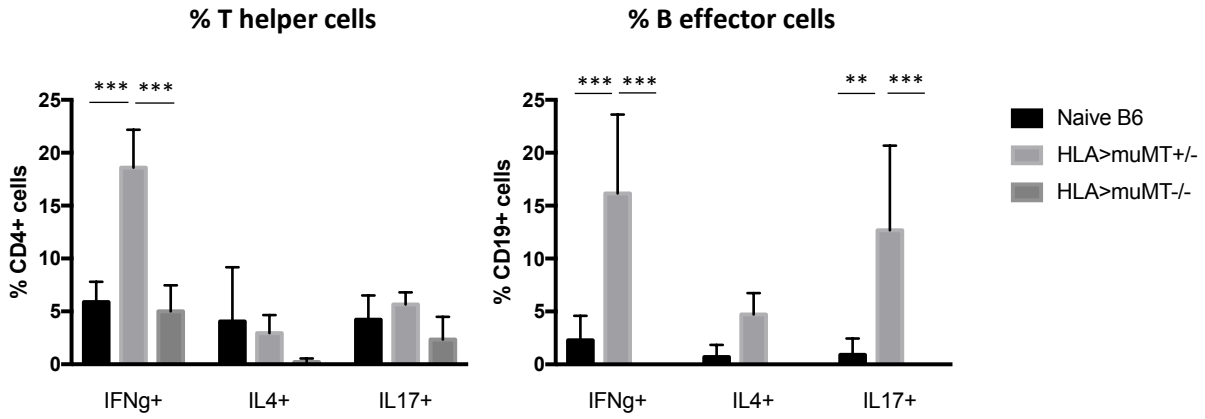

Fig. S6. Percentages of T helper and B effector responses in MLN from lung transplanted mice. Mediastinal lymph nodes (MLN) were mechanically dissociated, stimulated *ex vivo* with anti-CD3/CD28 (T helper cells) or anti-CD40+LPS (B effector cells) and analyzed by FACS after surface or surface and intracellular staining. Right: Cells producing IFNγ, IL-4 and IL-17A were expressed as % CD19+ cells and analyzed with a 2-Way ANOVA followed by a Bonferroni post-test. $^{**}p < 0.01$; $^{***}p < 0.001$. Left: Cells producing IFNγ, IL-4 and IL-17A (respectively reflecting Th1, Th2 and Th17 populations) were expressed as % CD4+ cells and analyzed with a 2-Way ANOVA with a Bonferroni post-test. $^{***}p < 0.001$.

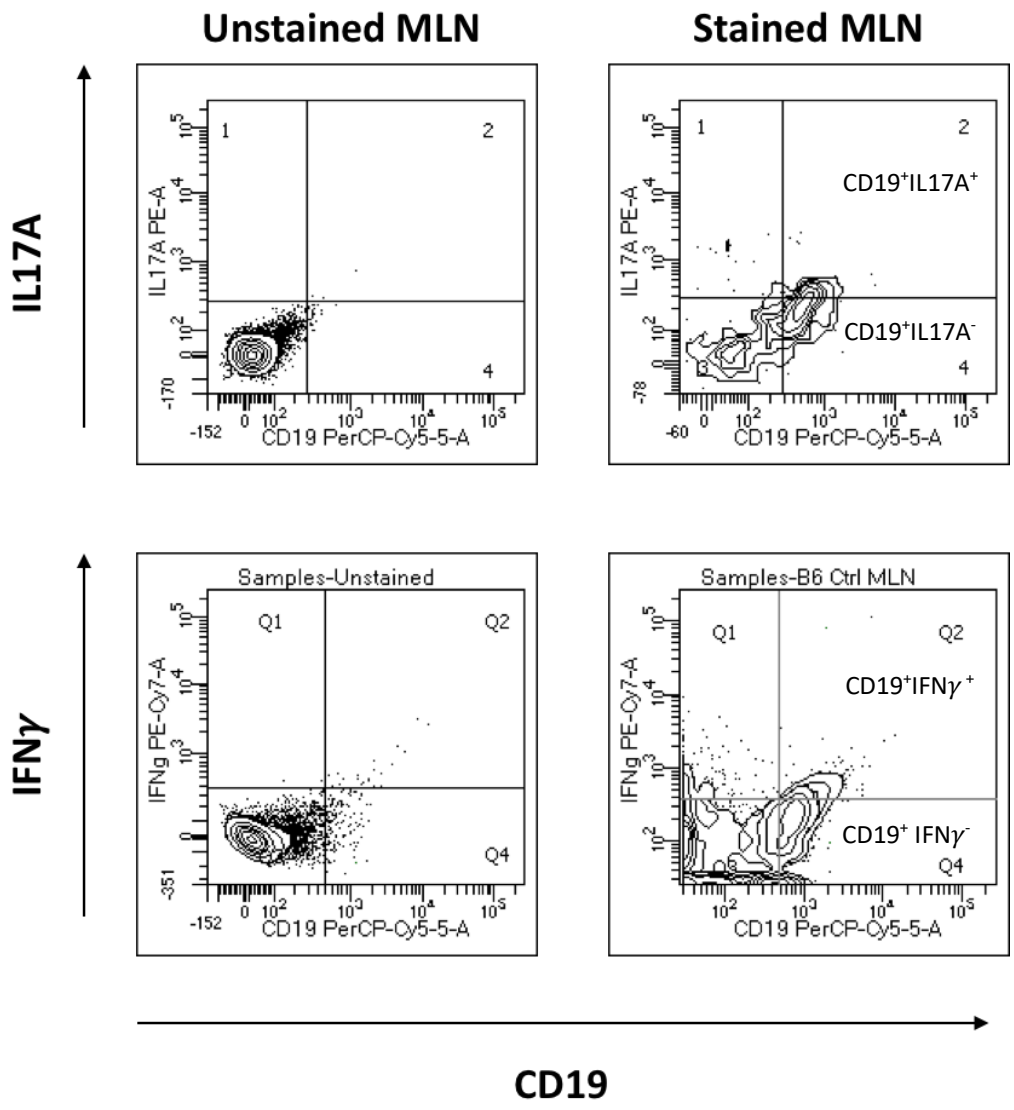

Fig. S7. Intracellular IFNg and IL17A in MLNs of lung transplanted rejecting mice. 2 months after orthotopic lung transplantation, MLNs were harvested, prepared as single cell suspensions and stimulated with anti-IgM overnight, before performing intracellular staining and flow cytometry analysis. Left panels: Unstained MLN cells show the baseline of flow cytometry detection. Right panels: MLN cells from HLA⟶μMT$^{+/-}$ LTx mice were stained for IL17A-PE and CD19-PerCP-Cy5.5 (top) and IFNγ -PE-Cy7 and CD19-PerCP-Cy5.5 (bottom).

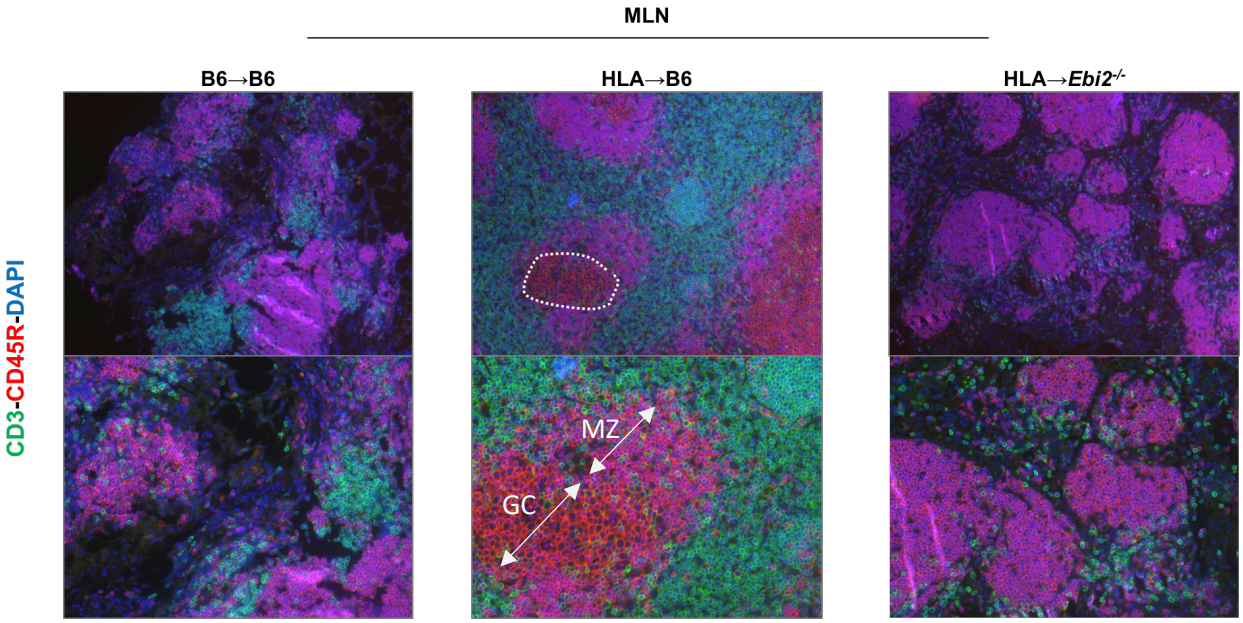

Fig S8. The formation of GCs in MLN is dependent on the HLA mismatch and on EBI2. Representative double immunofluorescence pictures of MLN harvested from B6→B6, HLA→B6 mice and HLA→EBI2$^{-/-}$ mice 2 months after lung transplantation, stained for CD3 (green) and CD45R (red). The white dotted outline shows a germinal center. The double-headed arrows delineate GC (germinal centre) and MZ (marginal zone) based on the morphology.

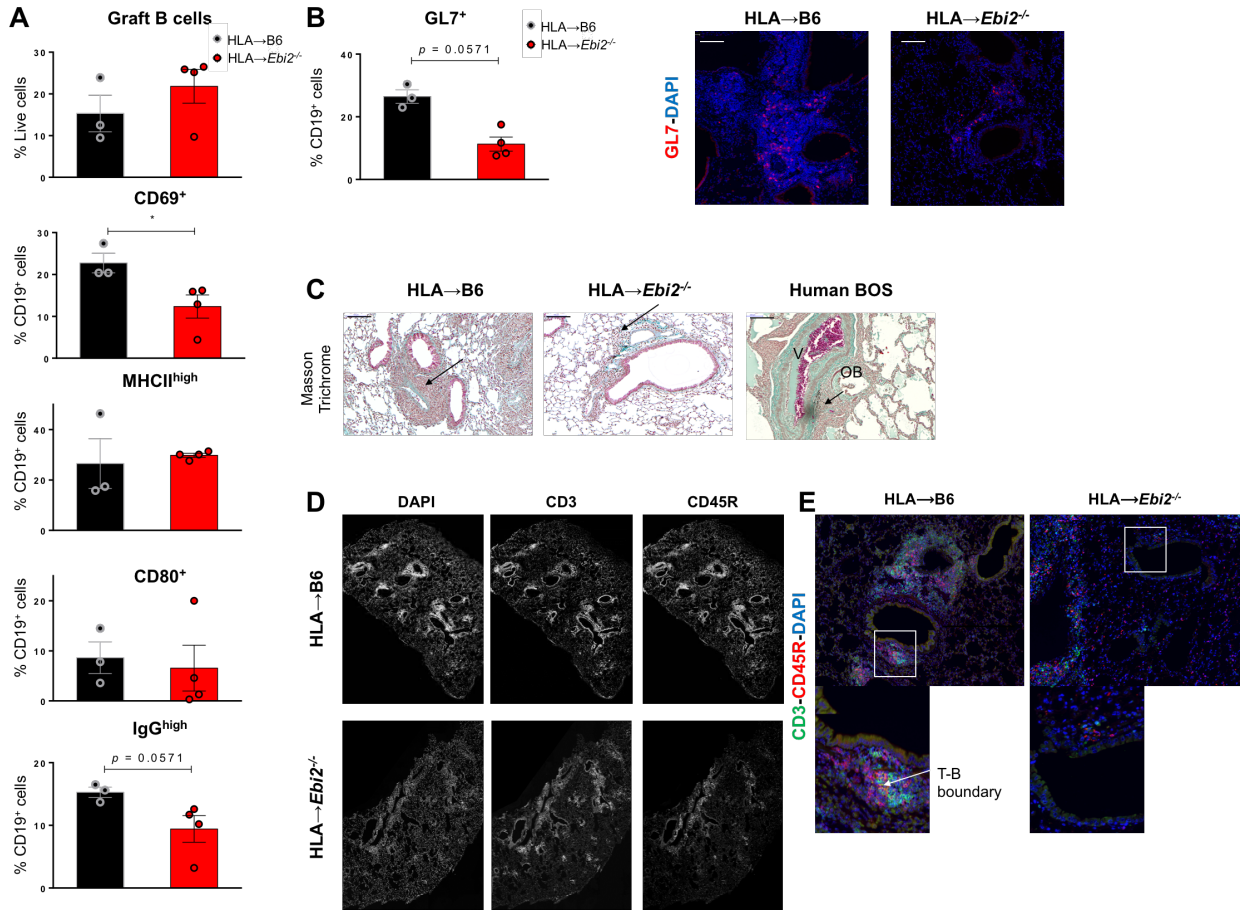

Fig S9. Ebi2 deficiency is associated with reduced B cell activation and follicle formation. (A) Quantification of CD19$^+$ B cells and CD69$^+$, MHCII^{high}, CD80$^+$, and IgG^{high} B cell populations in the lung grafts of indicated mice after flow cytometry. **(B)** Left: Quantification of the GL7$^+$CD19$^+$ cells in the lung grafts of indicated mice. Right: Representative immunofluorescence of lung grafts stained for GL7 (red) and counterstained with DAPI (blue). **(C)** Histological appearance of lymphoid follicles on Masson Trichrome-stained sections from indicated mice (left) and human BOS (right). **(D)** Scans of lung grafts, presented as single channels: DAPI, CD3 (T cells) and CD45R (B cells). **(E)** Representative immunofluorescence of peribronchial lymphoid follicles stained for CD3 (green), CD45R (red) and counterstained with DAPI (blue). Data are expressed as mean+/-SEM and analyzed a Mann-Whitney test. *p<0.05.